

ROLE OF RESIDUAL STRESSES ON MECHANICAL PROPERTIES
OF OBSIDIAN: NATURALLY OCCURRING GLASS

By

RAGHU V. MEESALA

Bachelor of Engineering in Mechanical Engineering
Osmania University
Hyderabad, India
2010

Submitted to the Faculty of the
Graduate College of
Oklahoma State University
in partial fulfillment of
the requirements for
the Degree of
MASTER OF SCIENCE
July, 2014

ROLE OF RESIDUAL STRESSES ON MECHANICAL PROPERTIES
OF OBSIDIAN: NATURALLY OCCURRING GLASS

Thesis Approved:

Dr. Raman P. Singh

Thesis Advisor

Dr. Kaan A. Kalkan

Dr. Hamed Hatami-Marbini

ACKNOWLEDGMENTS

Being a researcher has always been my dream. I would like to take this opportunity to thank my advisor Dr. Raman P. Singh who has been a great inspiration in my professional and personal life. I will always be indebted to him for allowing me to think independently.

I would like to thank Dr. Kaan A. Kalkan and Dr. Hamed Hatami-Marbini for their tremendous support and guidance. I also thank Dr. Sandip Harmikar and his student Seyyed Habib Alavi for allowing me to use the Vickers Indentator. Without the help of Dr. Teyler Ley and his student Mehdi Khanzadeh, working on XRF would have not been possible.

I would like to acknowledge my lab colleagues Arif, Kunal, Vijay, Hamim, Leila, Sanjay, Nitesh, Sandeep, Surendra and Vidyullatha for all their support during my life's highs and lows. Finally, I thank my father (Dr. M.Appalayya), mother (Ramadevi) and my sister (Nirupama) for their love and affection without which this achievement would not be possible.

”Acknowledgements reflect the views of the author and are not endorsed by committee members or Oklahoma State University.”

Name: RAGHU V MEESALA

Date of Degree: July, 2014

Title of Study: ROLE OF RESIDUAL STRESSES ON MECHANICAL PROPERTIES
OF OBSIDIAN: NATURALLY OCCURRING GLASS

Major Field: MECHANICAL AND AEROSPACE ENGINEERING

Obsidian is a natural glass of volcanic origin that is formed by the rapid cooling of viscous lava. Obsidian's mechanical properties in structure mechanics are visible in almost all aspects such as fracture pattern, elastic modulus, hardness and fracture toughness when compared to soda lime glass. Obsidian is currently used to produce scalpel blades and it forms sharper edges than any best surgical steel can do. The reason for the sharpness is speculated because of its structure and the way it fractures. Obsidian being an igneous rock, illustrates conchoidal fracture. As this natural glass cools very rapidly, the residual stresses in obsidian affects the way in which it fractures. This research is focused on the phenomena of residual stresses in obsidian and understanding the consequence of thermal annealing on the mechanical properties of obsidian. The indentation results indicated that obsidian has higher hardness than soda-lime glass. This work also compares the difference in the microstructure between obsidian and soda-lime glass. The presence of alumina is observed in obsidian. This study also shows the effect of thermal annealing on elastic properties of obsidian and its relation to residual stress. However, due to complex nature and structure of obsidian, any further research needs interdisciplinary efforts.

TABLE OF CONTENTS

Chapter	Page
I INTRODUCTION	1
I.1 Background	1
I.2 Motivation	3
I.3 Literature Survey	3
II EXPERIMENTAL DETAILS	6
II.1 Sample Preparation	6
II.2 SEM-EDS Analysis	7
II.3 X-ray Fluorescence	8
II.4 FTIR Analysis	8
II.5 Surface Roughness	9
II.6 Nanoindentation	9
II.7 Effect of Pile-up/Sink-in on Nanoindentation	10
II.8 Thermal Annealing	11
II.9 Differential Scanning Calorimeter	13
III RESULTS AND DISCUSSION	14
III.1 Composition: Obsidian vs Glass	14

III.2 Surface Roughness	18
III.3 Nanoindentation Results	19
III.4 Correction for Contact Area	20
III.5 Thermal Annealing Analysis	24
III.6 Effect of Residual Stresses	28
IV CONCLUSION AND FUTURE WORK	35
IV.1 Conclusion	35
IV.2 Future Work	36
BIBLIOGRAPHY	36

LIST OF TABLES

Table	Page
III.1 Elemental composition using EDS	14
III.2 Elemental composition using XRF	15
III.3 Oxide composition: obsidian vs glass	15
III.4 Surface roughness of obsidian	18
III.5 CSM indentation results	20

LIST OF FIGURES

Figure	Page
I.1 SEM image of obsidian blade	3
I.2 SEM image of metallic blade	3
II.1 Black obsidian	7
II.2 Obsidian used for nanoindentation	7
II.3 The semi-ellipse approximation technique [?]	11
II.4 Thermal annealing cycle	12
III.1 FTIR: obsidian vs glass	16
III.2 Scan size-1 μm^2	18
III.3 Scan size-25 μm^2	18
III.4 Scan size-100 μm^2	19
III.5 Load vs displacement	20
III.6 Modulus vs depth	20
III.7 Top view of the indent	21
III.8 Front view of the indent	21
III.9 Profile of X in Z direction	22
III.10 Profile of X in Y direction	22
III.11 Apparent Indentation modulus after area correction	22

III.12	Apparent Indentation hardness after area correction	23
III.13	Apparent Indentation modulus vs annealing temperature	25
III.14	Apparent Indentation hardness vs annealing temperature	26
III.15	Obsidian after thermal annealing at 900°C	27
III.16	DSC analysis of obsidian	28
III.17	Apparent Indentation modulus after area correction	29
III.18	Apparent Indentation hardness after area correction	30
III.19	SEM: Nanoindents around vickers Indent	31
III.20	Variation of apparent elastic modulus with distance from the indenter . .	32
III.21	Residual stresses variation in obsidian annealed at 500°C	33
III.22	Residual stresses variation in obsidian annealed at 800°C	34

CHAPTER I

INTRODUCTION

I.1 Background

Obsidian was discovered in Acheulian age around 1.5 million years ago [?]. Places with rhyolitic eruptions are the main source of obsidian. Obsidian is a naturally occurring glass is formed as an extrusive igneous rock, when volcanic lava cools rapidly [?]. In spite of their great significance to mankind through its involvement in most horrifying volcanic events, very little is known about it. Pre-Columbian Mesoamericans carved and worked on obsidian for making tools and decorative objects [?]. Obsidian was also used in making weapons, masks, jewelry and mirrors. Sourcing of obsidian plays a very important role in understanding the ancient civilizations [?]. Volcanic glasses once cooled do not devitrify unless they are subjected to heat or pressure. Obsidian when heated is vesiculated, that is it forms bubbles due to the release of volatiles. Due to this property it is generally used as light weight building material and fillers for composite light weight materials [?]. In archeological world, obsidian is used in a process known as bipolar reduction, wherein a piece of obsidian is placed on a hard anvil and smashed with a processor to produce sharp flakes that could be used for various cutting tasks.

Presently, obsidian is used to produce scalpel blades. It is very important to understand the degree of this sharpness. Obsidian is 210 to 1,050 times sharper than surgical steel,

100 to 500 times sharper than razor blade and 3 times sharper than diamond blade [?]. This was analyzed using lithic technology, through which a extremely sharp blade from the core of obsidian can be made. The cutting edge is a formed from a single fracture line, the edges measured through SEM are about 30 angstroms. At a magnification of 10000 times, the glass blade remains at a definite sharp blade where as razor blade is flat. The comparison between this edge and a razor blade was done by Buck [?]. Figure ?? shows an obsidian edge and figure ?? shows the edge of a metallic blade [?]. During surgical procedures the ragged edges of the metallic blade can entangle flesh in it whereas obsidian the edge is very sooth. So, it was widely used in surgical procedures. Disa *et al.* studied the efficiency of obsidian blades in wound healing of rats, these wounds also had less inflammation. Their study concluded that the scar width of the wounds caused by obsidian was significantly less than that caused by steel [?]. Obsidian's use as a scalpel was a rediscovery of the flint-knapping technique [?]. Flint-knappers produce a sharp edge of obsidian using controlled fracture. These sharp edges in obsidian are due to a type of fracture which is known as conchoidal fracture. This resembles a semicircular shell, with a smooth, and curved surface with no distinct planes and also occurs in flint, cubic zirconia and diamond. The fracture of this kind is generally associated with the flaws that occur in processing of the material. The amount of energy associated with crack propagation is related to the extent of crack branching which occurs extensively if large residual stresses or applied stresses exist. However, human clinical trials have not yet been approved by the US food and drug administration as obsidian is a natural glass and can have contamination or it can break during a surgical procedure. But it is always worthwhile to understand the reason behind the sharpness.

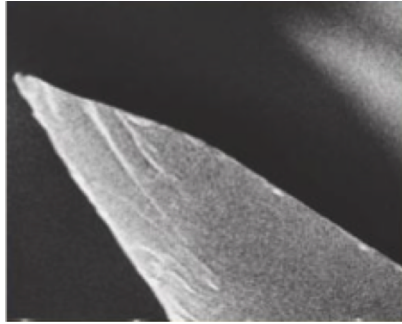


Figure I.1: SEM image of obsidian blade

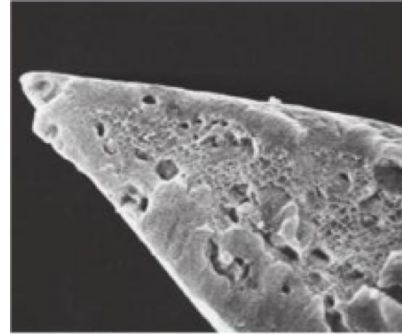


Figure I.2: SEM image of metallic blade

I.2 Motivation

To understand the relation between the structure of obsidian to its mechanical properties and to investigate the effect of thermal annealing on its mechanical properties. This study reports the behavior of residual stresses at these thermal annealing temperatures.

I.3 Literature Survey

Scientifically and technologically very little was known about obsidian as it requires an interdisciplinary approach. Geologists were interested in the archaeological origin of obsidian, hydration and fission track [? ?] whereas in medical industry obsidian was used to produce scalpels. Even though obsidian has quite a number of applications only few experimentalists were interested in the mechanical and chemical properties of obsidian. In 1924, George measured the Mohs scratch hardness, density and refractive index of some volcanic glasses [?]. This research was supported with an investigation on the chemical and physical properties of obsidian and they also compared the properties of obsidian

to pyrex and metallic glass [?]. Ericson *et al.* concluded that obsidian has high silica content than granite and has high hardness compared to silica glass. Gerth *et al.* were the first to investigate the mechanical properties of natural glasses using indentation methods, they reported the Young's modulus of obsidian using the Knoop hardness and Vickers hardness test [?]. Dorfman *et al.* investigated the mechanical and structural properties of obsidian and compared their fracture behavior to fused quartz [?]. They inferred that the segregation of its major chemical components have significant affect on its mechanical properties. Husien explored the micro-mechanical properties of obsidian and compared them with fused quartz. He concluded that the hardness of obsidian is greater than that of artificial glass [?].

Some high temperature and high pressure studies were conducted on obsidian. Matsushima *et al.* reported the elastic modulus of volcanic glass, glassy rocks and crystalline rocks at different temperatures [?]. Murase studied the visco-elasticity behavior and Young's modulus at higher temperatures [?]. Suito reported the elastic properties of obsidian under high pressure up to 6 GPa using ultrasonic technique [?]. It was observed that shear wave velocities in obsidian reach their minimum at 3.8 GPa and increase significantly up to 6 GPa. Asdelounis *et al.* studied the behavior of obsidian under scratch test [?]. Ma *et al.* studied the origin of color in obsidian and analyzed their spectroscopic properties. They suggested that the transmission color of obsidian is due to the presence of Fe^{3+} and Ti^{3+} even though the oxidation state of Ti is still debatable [?]. High temperature studies on obsidian helped reconstruct fire histories. The hydration bands of obsidian establishes pre-historic site chronologies and depositional integrity [?]. Kolzenburg *et al.* observed that the mechanical behavior of a glass is determined by its thermal and

stress history after it has crossed the glass transition temperature. They also concluded that heat treatment of obsidian affects the mechanical properties of the natural glass and it has higher post-fragmentation strengths than glass [?]. This study also mapped the topography, modern features, areas of burning and division of clusters in archeological sites into eight different categories. Shackley *et al.* analyzed the thermal behavior of obsidian in a controlled environment and concluded that the chemical composition of this natural glass is not altered by high annealing temperature [?].

CHAPTER II

EXPERIMENTAL DETAILS

II.1 Sample Preparation

Figure ?? shows a sample of obsidian which was obtained from Wards Natural Science Establishment (Rochester, NY). The color of obsidian is due to the presence of different elements like Fe and Mg in very little quantities [? ?]. Quite strangely, it appears in other different colors depending on the direction in which it is cut. When cut in one direction it is jet black whereas in another direction, it is gray. In this research obsidian, (79.26% SiO₂, 12.41% Al₂O₃, 4.14% Na₂O, 3.98% K₂O, 1.47% Fe₂O₃, 0.35% CaO, 0.11% TiO₂, 0.05% MgO) [?] was compared with a reference material which has similar silica content. The reference material was a glass slide (73% SiO₂, 2% Al₂O₃, 14% Na₂O, 7% CaO, 4% MgO) of Type II as per A.S.T.M. - 438 federal spec DD-G-54lb [?]. These reference samples were obtained from Thermo Fisher Scientific Inc.

Obsidian rock was cut using a precision saw (Isomet 1000) and later sliced to flat 5 mm samples using a diamond blade on a low speed cutting saw (Struers Minitom). Standard metallographic techniques were used to polish the samples. Figure ?? shows the polished obsidian samples in a nanoindentation test. Few samples show snowflake pattern, which is generally attributed to the presence of cristobalite. For T_g measurements, very small samples weighing less than 10 mg were used.



Figure II.1: Black obsidian

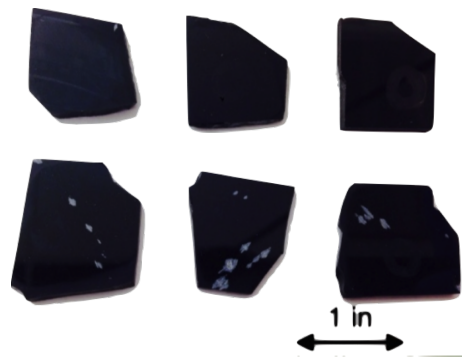


Figure II.2: Obsidian used for nanoindentation

II.2 SEM-EDS Analysis

Scanning Electron Microscopy (SEM) was employed for high magnification imaging of obsidian. Hitachi S-4800 Type II Ultra-High resolution field emission scanning electron microscope (GCETMarket, Inc., Blackwood, NJ) was used. Energy dispersive X-ray spectroscopy (EDS) was used to analyze the elemental compositions in obsidian. Obsidian being a non-conducting material was coated with gold/paladium to prevent charging while performing SEM-EDS.

II.3 X-ray Fluorescence

X-Ray Fluorescence is a very powerful technique when compared to EDS. A lot of research has been done on sourcing of obsidian using XRF. It was basically used to study archaeological specimens and obsidian artifacts. A X-ray fluorescence (Edax Inc., Mahwah, NJ) instrument was used to analyze the glass samples. To efficiently excite the elements from Fe to Mo X-rays from 17 keV to 40 keV were focused on the sample. The other advantage of XRF is that no coating of glass samples was required.

II.4 FTIR Analysis

InfraRed spectrum represents a fingerprint region, which is unique to the material. This region has absorption peaks which relate to the frequencies of vibrations between bonds. A Fourier Transform equation is used to get the full spectrum. In addition to the identification of bonds, spectroscopy indicates the amount of material present in the form of peaks. Attenuated Total Reflectance - Fourier Transform InfraRed (ATR-FTIR) was utilized to acquire spectra of obsidian and glass using FTIR Varian 680-IR Spectrometer and Cary 600 Series FTIR Microscope (Agilent technology, Santa Clara CA). The spectra was collected between 1400, and 400 cm^{-1} using a diamond probe. Samples were subjected to 32 scans at a resolution of 4.0 cm^{-1} . A temperature of 28°C was maintained during the experiment. The sample surfaces were made flat to avoid noise due to surface roughness.

II.5 Surface Roughness

The surface roughness of obsidian was calculated using Atomic Force Microscopy (Asylum Research MFP- 3D). AC 240 tip, made of silicon was used in contact mode. Obsidian samples were held on glass slides during experimentation. A 3D profile on nanoscale was obtained by measuring the forces between the sharp probe and the surface at a very close distance. The cantilever tip records small force between the probe and surface in contact [?].

II.6 Nanoindentation

Nanoindentation is a commonly used method to determine the elastic modulus and hardness of an unknown material [?]. This method is generally used to determine the properties at nano level. Experiments were performed on a Nanoindenter XP system (MTS Systems Corporation, USA) using CSM Hardness, Modulus and Tip Calibration. Continuous Stiffness Measurement (CSM) method is a well-established technique for obtaining elastic modulus and hardness data continuously during nanoindentation [?]. Due to the high frequency of the oscillations used, CSM is less sensitive to thermal drifts. CSM can be used to measure properties continuously during the indentation process instead of discrete unloading cycles [?].

Mechanical properties of obsidian are determined using Berkovich tip. The analysis with this tip could be used to correlate the theories on elasticity. When compared to a four sided Vickers indenter, Berkovich tip is more sharper ensuring precise control over indentation process. The values $E_{indenter} = 1141$ GPa, $\nu_{indenter} = 0.07$ and $\nu_{obsidian} = 0.18$ where ν

denotes Poisson's ratio and E denotes elastic modulus are used in all computations.

II.7 Effect of Pile-up/Sink-in on Nanoindentation

During the elastic-plastic indentation, a zone of plastically deformed material may extend beneath the indentation and around the perimeter of contact [?]. Kinematics of indentation process involves the presence of primary slip in the local deformation around the indent. Dominance of this primary slip at the intersection of primary slip direction and the indented surface gives rise to pile-up. Plasticity in a material is understood with the amount of pile-up or sink-in at the surface during indentation. Not accounting for pile-up leads to underestimation and/or overestimation of the contact area, which results in erroneous elastic modulus and hardness. Ratio of the residual depth of the indentation to the total depth, h_f/h_{max} was a critical factor in predicting pile-up [?]. Numerous methods were introduced to correct pile-up. Truck *et al.* introduced a technique which utilizes the information on the energy dissipated during the indentation to determine mechanical properties [?]. As this method was less sensitive to the effect of pile-up, Hertzian loading analysis method was employed to correct hardness and elastic modulus. This method calculates the pile-up contact area by relating the contact depth to the contact radii. In this research the indents were scanned after indentation to correct for pile-up [?]. This method can be compared to Atomic Force Microscopy with the only difference being that it has a very low compliance. Equations ?? and ?? were used for calculation of pile-up where $A_{Oliver-Pharr}$ is the area obtained from Oliver-Pharr model of load-displacement graphs, $A_{Pile-up}$ is the area obtained upon pile-up, h_c is the depth of indentation and coefficients a_i give the height of pile-up in three directions. A Berkovich tip was used for all

calculations, figure ?? depicts the schematic of the tip where a is the contact perimeter, L is the pile-up height, b representing the side of the indent. These parameters also depend on the indenter geometry and the depth of indentation.

$$A_{true} = A_{Oliver-Pharr} + A_{Pile-up} \quad (II.1)$$

$$\Delta A = A_{true} - A_{Oliver-Pharr} = 1.923h_c \sum a_i \quad (II.2)$$

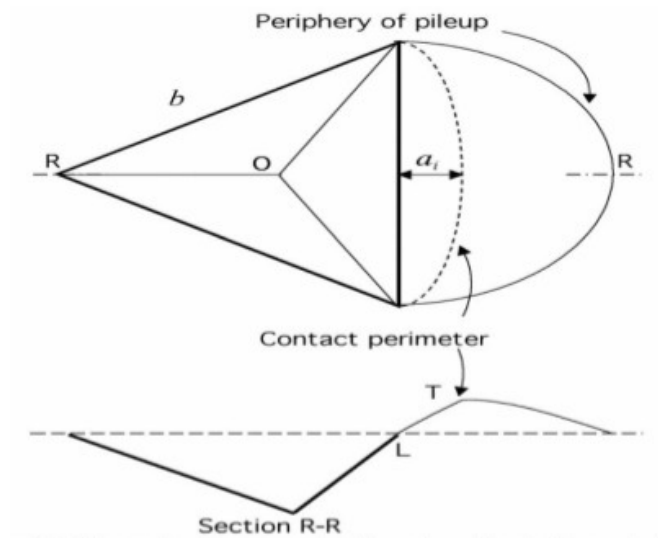


Figure II.3: The semi-ellipse approximation technique [?]

II.8 Thermal Annealing

Annealing is a process of heating glass samples uniformly and holding it at temperature long enough to remove all stresses caused from manufacturing process or thermal history.

Soaking time also called as holding time plays a very important role in annealing. Soaking time is the amount of time at which the material is heated in the tube furnace. Shorter soaking time at a lower temperature may not relieve all the stresses present in glass. Thermal annealing was performed in a Sentrotech tube furnace. Glass samples were cooled very slowly as the surface and interior regions cool at different rates. To prevent oxidation, thermal annealing was performed maintaining inert atmosphere. The obsidian and soda-lime glass samples were weighed and examined for physical changes. The samples were subjected to a thermal annealing cycle as shown in figure ???. The samples were initially heated to a certain temperature, soaked for 2 hours and later were cooled down slowly to room temperature. After every thermal annealing session, SEM-EDS analysis was done. The samples were subjected to six heating sessions starting from 300°C to 800°C. The heating rate was 5°C/min and cooling rate was 3°C/min.

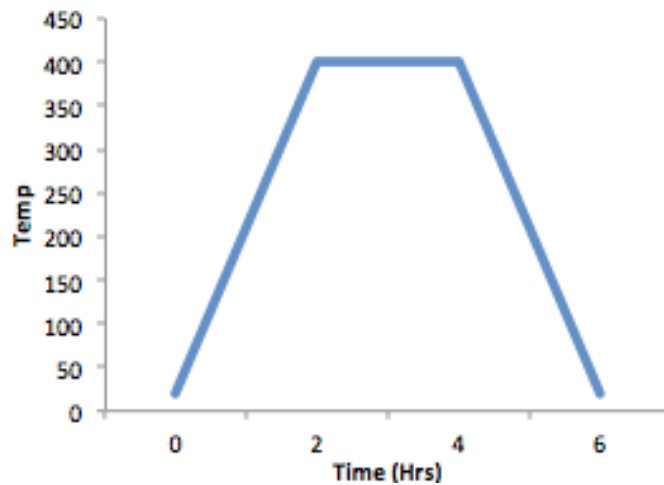


Figure II.4: Thermal annealing cycle

II.9 Differential Scanning Calorimeter

Differential Scanning Calorimetry is a thermo-analytical technique, in which the sample and reference are heated to a certain temperature and the difference in the amount of heat required to raise the temperature by one degree is measured as a function of temperature. Using DSC exothermic or endothermic reactions can be identified. DSC curve can also be used to calculate the enthalpies of transition. Thermal behavior of obsidian was studied using a Netzsch STA 449 F1(Jupiter) under constant flowing argon. Less than 10 mg of obsidian samples are loaded on to the aluminum pan. Thermal analysis has been performed to determine the changes in mass and caloric reactions in the temperature range of 25°C to 1200°C. To obtain T_g , the samples were heated to 1200°C at a scan rate of 10°C/min, held at that temperature for 5 min, to eliminate any previous thermal history and then cooled slowly to room temperature.

CHAPTER III

RESULTS AND DISCUSSION

Husein's work reported that fracture toughness of obsidian is twice that of glass and Dorfman et al., related this behavior to compositional change [12]. So, this study analyzed the compositional difference and similarities between obsidian and soda-lime glass.

III.1 Composition: Obsidian vs Glass

Elemental composition of obsidian and soda-lime glass was determined with SEM-EDS analysis. Table 3.1 shows the average elemental compositions of ten obsidian samples and it is inferred that obsidian has high percentage of aluminum content when compared to soda-lime glass. From table 3.1 it can be inferred that soda-lime glass has high percentage of sodium which is added to the glass during production to lower the melting point. To comprehend and support these results, a more powerful technique like XRF is required.

Table III.1: Elemental composition using EDS

Sample	Si (wt%)	O (wt%)	Al (wt%)	K (wt%)	Na (wt%)
Obsidian	38.4 ± 0.1	41.1 ± 0.3	6.8 ± 0.1	4.2 ± 0.5	2.3 ± 0.3
Soda Lime Glass	35.2 ± 0.8	47 ± 0.4	0.9 ± 0.1	1.4 ± 0.2	10.5 ± 0.8

XRF was performed to support the observations of EDS on glass samples. Table ?? shows the elemental compositions of the two glasses. It can be observed that the XRF data does not show elemental composition of oxygen as it is unable to quantify lighter elements in the periodic table. Obsidian and glass show traces of Ti and Mn, the only difference being that obsidian shows presence of Fe. Obsidian is black in color due to presence of Fe whereas soda-lime glass is optically clear as it has no Fe composition. Oxides percentages in table ?? confirm the presence of alumina in obsidian.

Table III.2: Elemental composition using XRF

Sample	Na (wt%)	Mg (wt%)	Al (wt%)	Si (wt%)	K (wt%)	Ca (wt%)	Fe (wt%)
Obsidian	6.1 ± 0.1	0.3 ± 0.1	10.5 ± 0.2	71.0 ± 0.3	9.1 ± 0.2	1.3 ± 0.2	1.3 ± 0.1
Glass	17.3 ± 0.2	5.9 ± 0.1	1.5 ± 0.1	64.2 ± 0.1	1.6 ± 0.1	9.3 ± 0.1	0.04 ± 0.01

Table III.3: Oxide composition: obsidian vs glass

Sample	Na ₂ O (wt%)	MgO (wt%)	Al ₂ O ₃ (wt%)	Si ₂ O ₃ (wt%)	K ₂ O (wt%)	CaO (wt%)	Fe ₂ O ₃ (wt%)
Obsidian	6.0 ± 0.2	0.3 ± 0.1	10.5 ± 0.3	71.0 ± 0.5	9.1 ± 0.2	1.2 ± 0.3	0.1 ± 0.2
Glass	18.2 ± 0.2	6.0 ± 0.1	1.5 ± 0.1	69.1 ± 0.7	1.6 ± 0.1	4.4 ± 0.1	0.02 ± 0.01

Field strength of aluminum is greater than sodium and potassium based on network theory of Dietzel [?]. Hence, aluminum can form a bond with oxygen and replace silicon in the hierarchical structure. Two major observations have been inferred from EDS data: (i) There are Si-O-Si bonds in soda-lime glass whereas Si-O-Al bonds in obsidian (ii) It is also observed that the oxygen to silicon ratio in obsidian is less than that of glass. For

better understanding of the bonds in these samples, Fourier Transform InfraRed (FTIR) was performed.

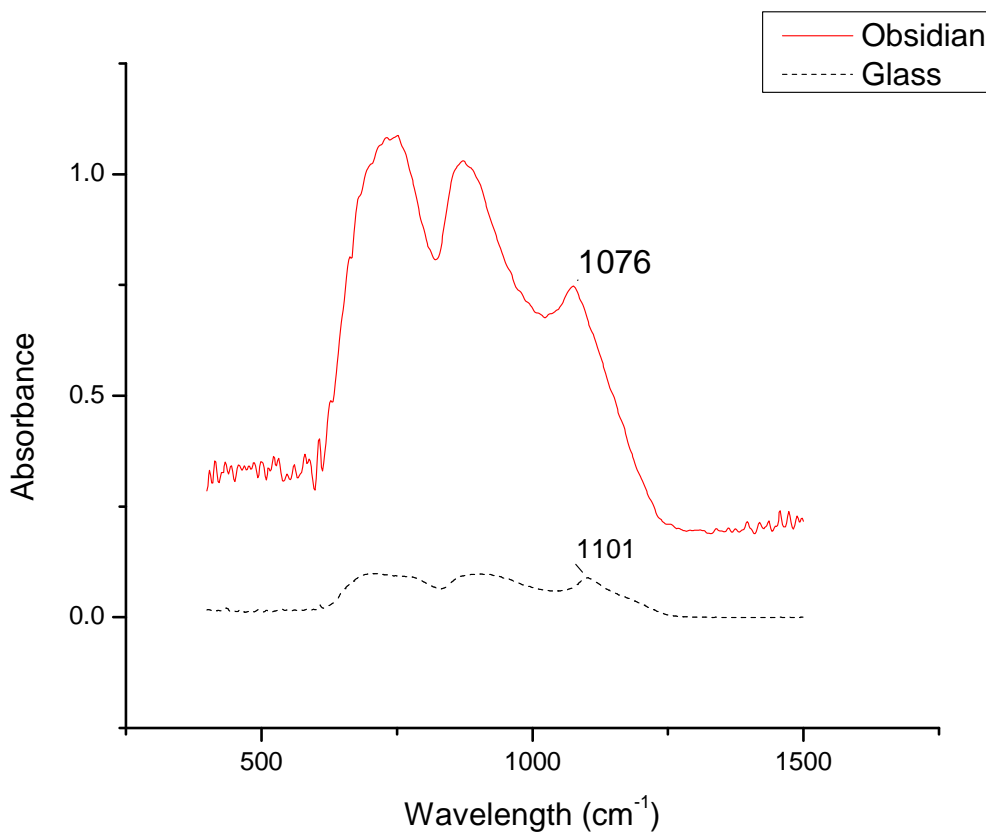


Figure III.1: FTIR: obsidian vs glass

Figure ?? shows the Fourier Transform InfraRed (FTIR) absorption spectra of obsidian and glass investigated between 1400, and 400 cm^{-1} . FTIR spectra of glass has three absorption bands around 725, 860, and 1086 cm^{-1} whereas obsidian has three absorption bands around 720, 865, and 1101 cm^{-1} . The peak around 720 cm^{-1} is assigned to Si-O-Si symmetric stretching of bridging oxygens, the peak around 860 cm^{-1} is assigned to Si-O

stretching of non-bridging oxygens. Significant peak shift between obsidian and soda-lime glass is observed for the third absorbance peak. This shift can again be explained with the theory of Dietzel. Pure silica asymmetric vibration is around 1110 cm^{-1} and as the network formers in obsidian are only Al and Si, the substitution of Al amongst Si-O-Si network will reduce the stretching wave number [?]. Al being the second neighbor to Si, will attract more oxygen atoms than Si. Hence, the asymmetric stretching wavenumber of Si-O-Al will be located at a lower wavenumber than Si-O-Si. The shift can also be reasoned due to the fact that atoms of higher mass vibrate at lower frequencies than the bonds between lighter mass atoms [?]. Equation ?? shows a relation between wavelength and reduced mass where ν is the natural vibration of the bond, c is the velocity of light, k is a constant which varies from bond to bond and μ is the reduced mass.

$$\nu = \frac{1}{2\pi c} \sqrt{\frac{k}{\mu}} \quad (\text{III.1})$$

Condon-Morse model validates that modulus is influenced by the dimensionality and connectivity of the structure [?]. Based on the hardness values of alumina and silica, alumina has a hardness of 3 on Mohs scale and silica has a hardness of 6 - 7 on Mohs scale. So, compositional change cannot be the only factor which controls these properties. To understand this better fundamental mechanical characterization on obsidian was performed.

As the mechanical characterization of obsidian was done at nanoscale, it is very important to check if the surface roughness of obsidian is within limits.

III.2 Surface Roughness

To understand the structure property relation for obsidian, preliminary experiments have been performed to determine its mechanical properties. Surface roughness can affect the results of nanoindentation, so obsidian samples were imaged using Atomic Force Microscopy (AFM) and surface roughness was calculated.

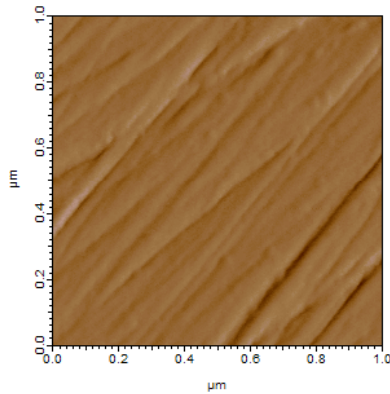


Figure III.2: Scan size-1 μm^2

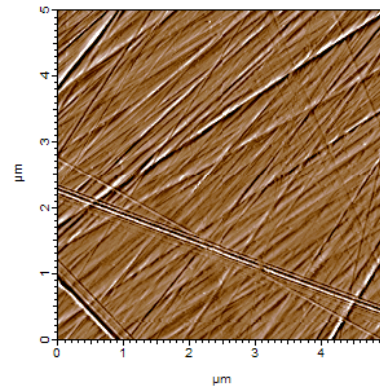


Figure III.3: Scan size-25 μm^2

Table III.4: Surface roughness of obsidian

Scan size (μm^2)	RMS value (nm)
1.0	1.789
25.0	1.790
100.0	1.785

Figure ??, ?? and ?? show the surface of obsidian for different scan areas of 1 μm^2 , 25 μm^2 , 100 μm^2 respectively. The RMS values of surface roughness for the three scanned areas are shown in table ?. The average RMS value of surface roughness was determined to be 1.7 nm which is less than 1/10th the indentation depth. So it can be inferred that

surface roughness does not affect the mechanical properties.

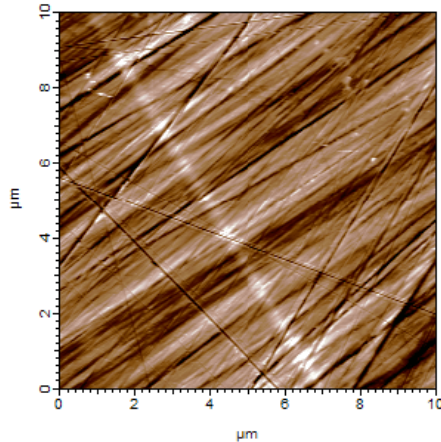


Figure III.4: Scan size-100 μm^2

III.3 Nanoindentation Results

The calculated indentation modulus and hardness by the CSM technique of nanoindentation are shown in table ???. These values were an average of ten different samples with fifty indents on each of them. Figure ??? shows a typical load vs displacement graph for obsidian. To calculate the elastic modulus, the values were calculated for an average of 200 to 1000 nm. The variation of modulus with respect to displacement for two indents is depicted in figure ???. The maximum depth of these indents is 1500 nm. The elastic modulus and hardness values are in agreement with literature [? ?]. The results show that the hardness of obsidian is greater than glass. As indentation involves plasticity, it is interested to check if the residual image of obsidian shows any change in contact area due increase or decrease in plasticity.

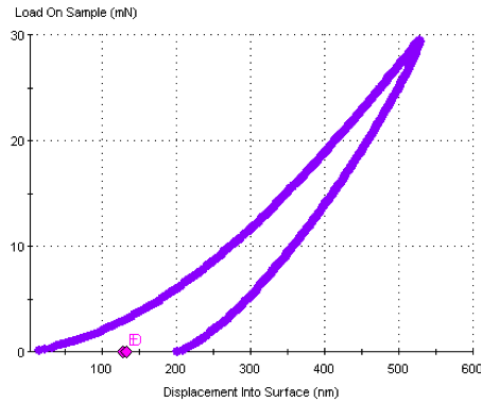


Figure III.5: Load vs displacement

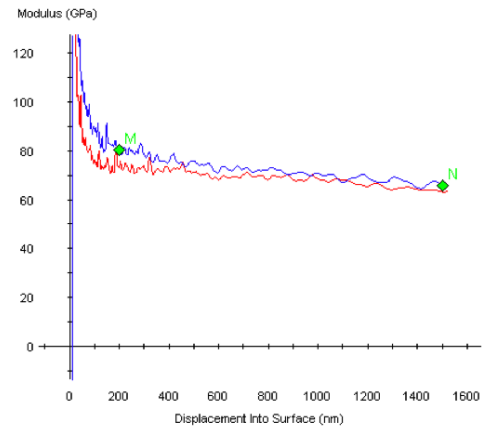


Figure III.6: Modulus vs depth

Table III.5: CSM indentation results

Sample	Indentation Modulus (GPa)	Indentation Hardness (GPa)
Obsidian	72 ± 3	6.5 ± 0.3
Soda Lime Glass	68 ± 2	5.5 ± 0.4

III.4 Correction for Contact Area

Obsidian is a volcanic rock which cools very rapidly [?], whereas an artificial glass is generally manufactured upon slow cooling. As, the thermal history of a material is a critical factor in deciding pile-up or sink-in behavior during indentation [?] one can expect such behavior in obsidian. In nanoindentation, the mechanical properties will depend on the amount of stress which is applied on the surface. The amount and nature of stress will decide the shear stress beneath the indenter. This shear stress drives the plasticity which in turn causes pile-up or sink-in in materials. Generally, compressive stresses lead to large pile-up whereas pile-up is smaller for tensile stresses. Bolshakov *et al.* reported the dependence of mechanical properties on applied or residual stress [?]. Pile-up and sink-in

leads to apparent indentation elastic modulus and hardness.

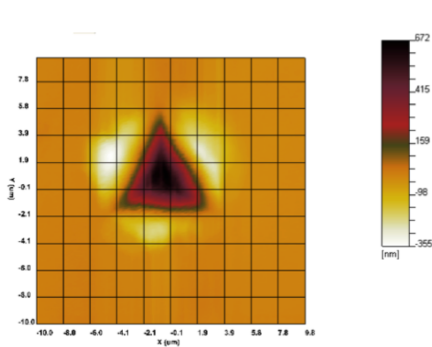


Figure III.7: Top view of the indent

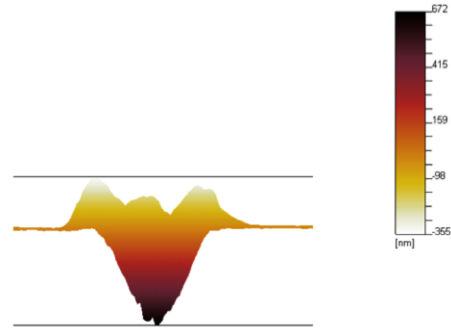


Figure III.8: Front view of the indent

In this study, nanovision technique of nanoindentation was used in correcting the contact area. Figure ?? and ?? show the top and front view of the indent respectively. Figure ?? clearly shows the pile-up in obsidian. Profiling the top view in X and Y direction, figure ?? and ?? are used to find the coefficients a_1 , a_2 , a_3 of equation ?? . These coefficients are used to calculate the pile-up area. The co-efficients and pile-up area calculated are used in the equations ?? and ?? , to determine ΔA . Using the A_{true} , the apparent elastic modulus and hardness of obsidian were calculated [?]. Figure ?? and ?? show the variation of apparent indentation modulus and hardness of obsidian with reference to the indent number respectively. Based on these plots we can conclude that apparent indentation modulus and hardness are decreased with the affect of pile-up.

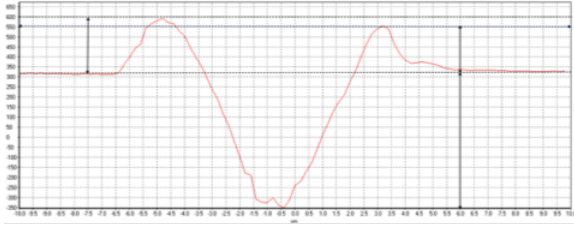


Figure III.9: Profile of X in Z direction

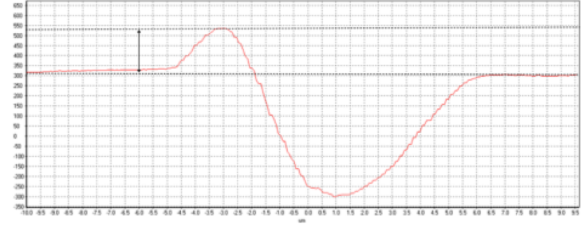


Figure III.10: Profile of X in Y direction

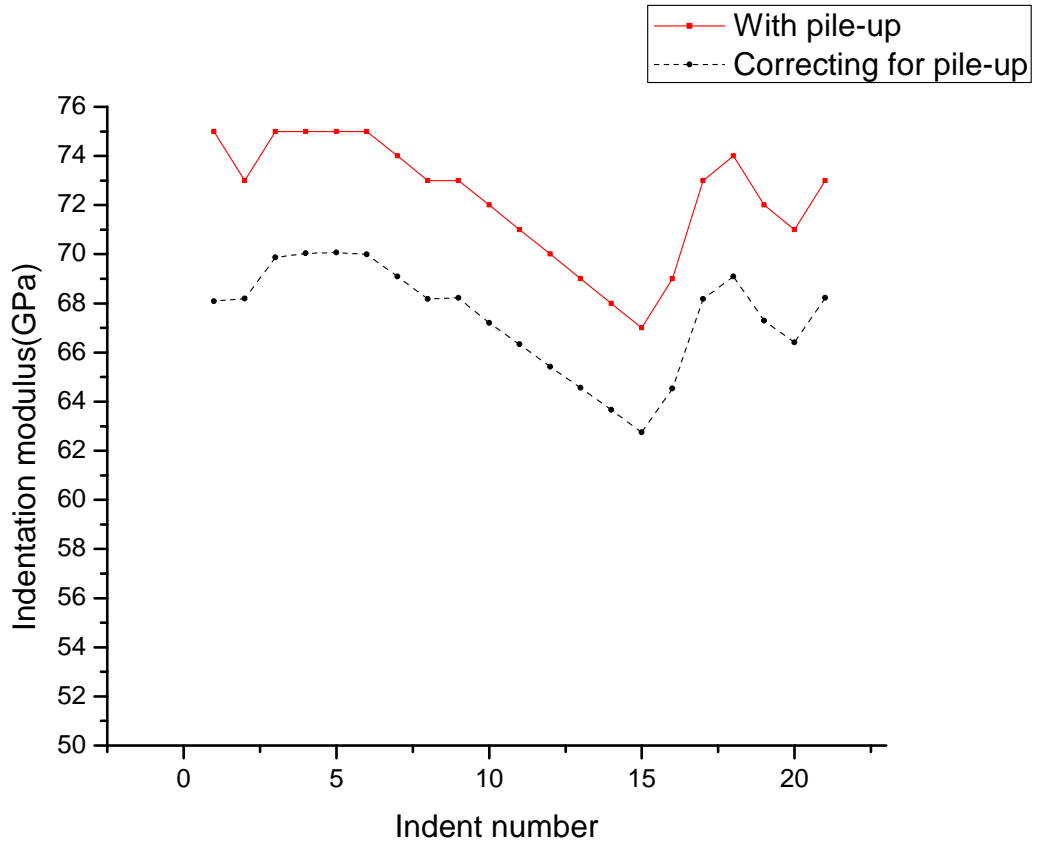


Figure III.11: Apparent Indentation modulus after area correction

A simple experiment was performed to understand the difference between as received obsidian and glass samples. Both the samples were heated to 500 °C and quenched it

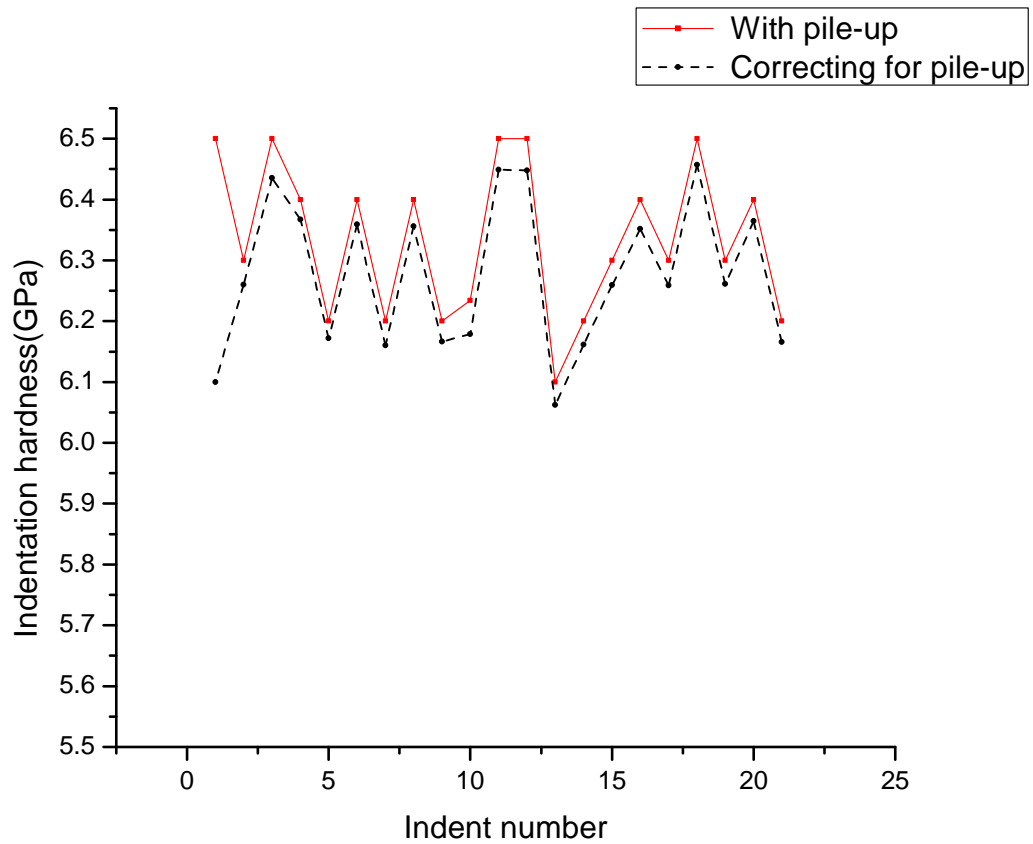


Figure III.12: Apparent Indentation hardness after area correction

rapidly in a tub of water. It is seen that soda-lime glass has shattered upon contact with water whereas obsidian samples have not shattered. Obsidian can take bigger thermal shock when compared with soda-lime glass. There can be stresses generated as all the layers in the glass samples do not cool at the same rate. This differential cooling process can lead to residual stresses. This experiment gives us insight that obsidian is a stronger material as it is rapid cooled when compared to soda-lime glass based on its thermal history.

III.5 Thermal Annealing Analysis

To understand the role of residual stresses in obsidian and soda-lime glass, these samples have been thermally annealed to different temperatures. Figures ?? and ?? show the variation of indentation modulus and hardness with annealing temperature. It is observed that there is a decrease in elastic modulus and hardness when both the glasses have been thermally annealed. A greater decrease of elastic modulus and hardness in soda-lime glass is noticed after 500 °C. To explain this behavior it is very important to determine the transition temperature of obsidian.

After every thermal annealing cycle, SEM-EDS was performed to check for compositional changes. Obsidian and glass showed no compositional change, which fact is validated by this study; this is consistent with literature [?]. FTIR also showed no shift in peaks after thermal annealing. There were no physical changes until 600°C. At 700 °C obsidian showed a white discoloration and at 800°C thermal cracking and minor vesiculation was observed. At 900°C the obsidian sample completely vesiculated as shown in figure ??, this is due to off-gassing. After 700°C the soda-lime glass started to bend and melt so indentation measurements were not possible after this temperature.

Differential Scanning Calorimetry (DSC) was performed to determine the glass transition temperature of obsidian. Glass transition temperature is that temperature at which there is a change of slope for the specific volume versus temperature curve. Figure ?? shows the glass transition temperature of obsidian to be around 800°C. The glass transition temperature of soda-lime glass was measured to be 530°C [? ?]. As the T_g of glass is lesser than that of obsidian we have seen a greater decrease in mechanical properties at 500°C.

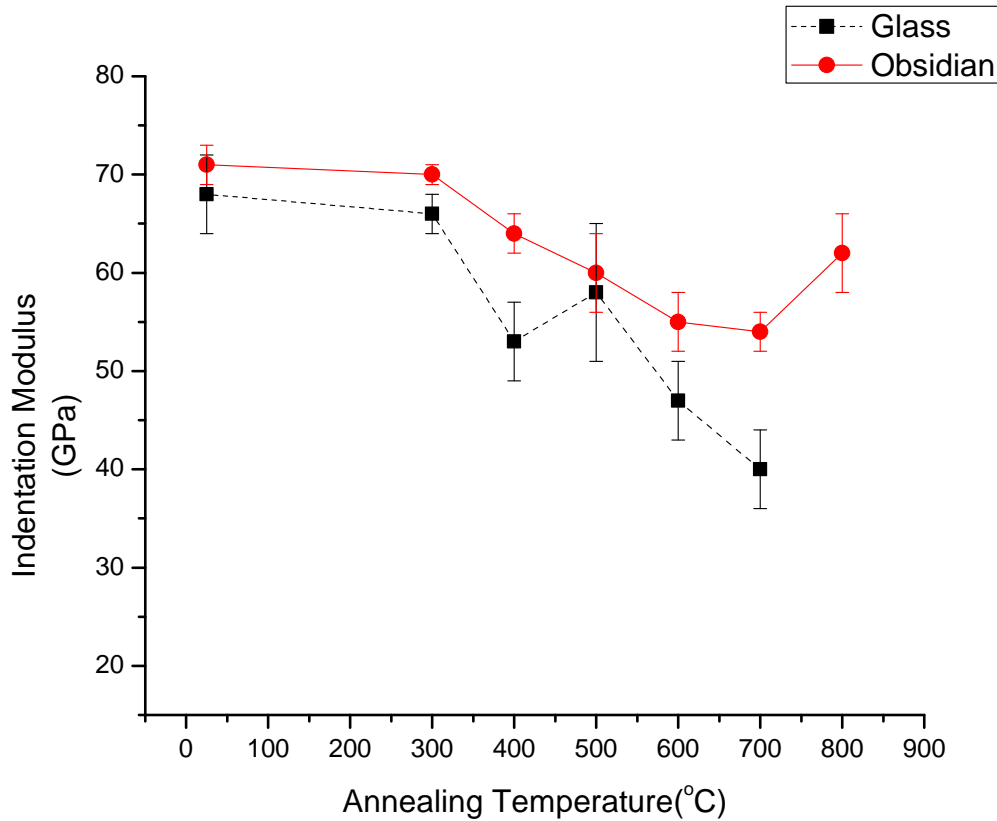


Figure III.13: Apparent Indentation modulus vs annealing temperature

This decrease in elastic modulus and hardness upon thermal annealing may be apparent as the measurement of mechanical properties by indentation involves the factor of contact area. This also can be explained due to the fact that the elastic modulus being an inherent property of a material and should not be influenced by stress [?]. Bolshakov *et al.*, proved in his study that contact area calculated from nanoindentation is incorrect if there are residual stresses present in the material. Residual stresses can be both compressive and tensile in nature. Force generated by the indenter generates a shear stress which can be

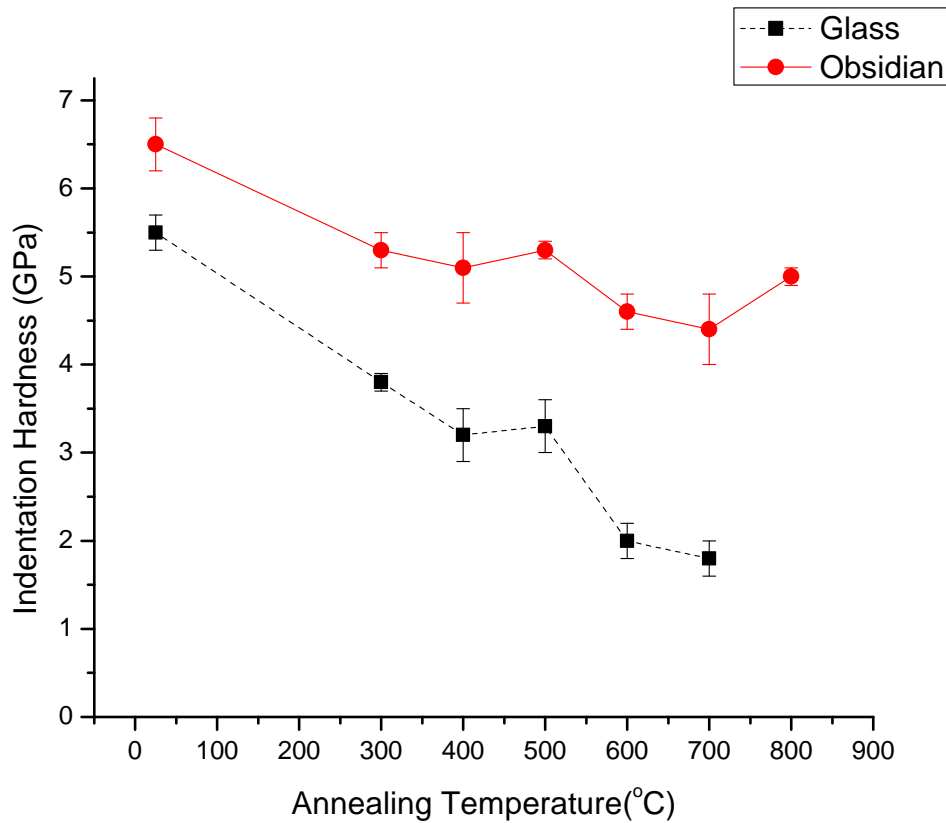


Figure III.14: Apparent Indentation hardness vs annealing temperature

either tensile or compressive in nature. The tensile stress enhances the shear stress beneath the indenter whereas compressive stress will reduce the shear stress. The plasticity beneath the indenter is affected by these shear stresses and it is shown in form of pile-up and sink-in [? ?]. Residual stresses indirectly affect the contact area as they affect the plastic deformation during indentation [? ?]. Phar *et al.* showed that stresses affect the hardness and elastic modulus which indirectly affects the contact area, which helps us validate our experiments [?].



Figure III.15: Obsidian after thermal annealing at 900°C

To correct for pile-up or sink-in, the calculations detailed earlier were used. There might be a chance that strain hardening in obsidian is causing the material to be displaced far away from indentation and resulting in sink-in [?]. Figure ?? shows the final elastic modulus after correction whereas ?? shows the variation of indentation hardness after correction. An effect of annealing is to increase the nanoindentation elastic modulus [?]. An increase in elastic modulus is observed at after T_g . This shows that soaking time plays an important role in annealing. As the soaking time in these experiments is only two hours, the stresses may not be completely released in obsidian when it is heated to a temperature below T_g . Also figure ?? shows that the apparent elastic modulus increases at 800°C after correction for pile-up. This also might be the effect of residual stresses in obsidian. As this temperature is close to T_g , annealing for two hours can completely relieve stress which might cause an increase in modulus and hardness. To understand the role of residual stresses we need to quantify the stresses with change in annealing temperature and soaking time.

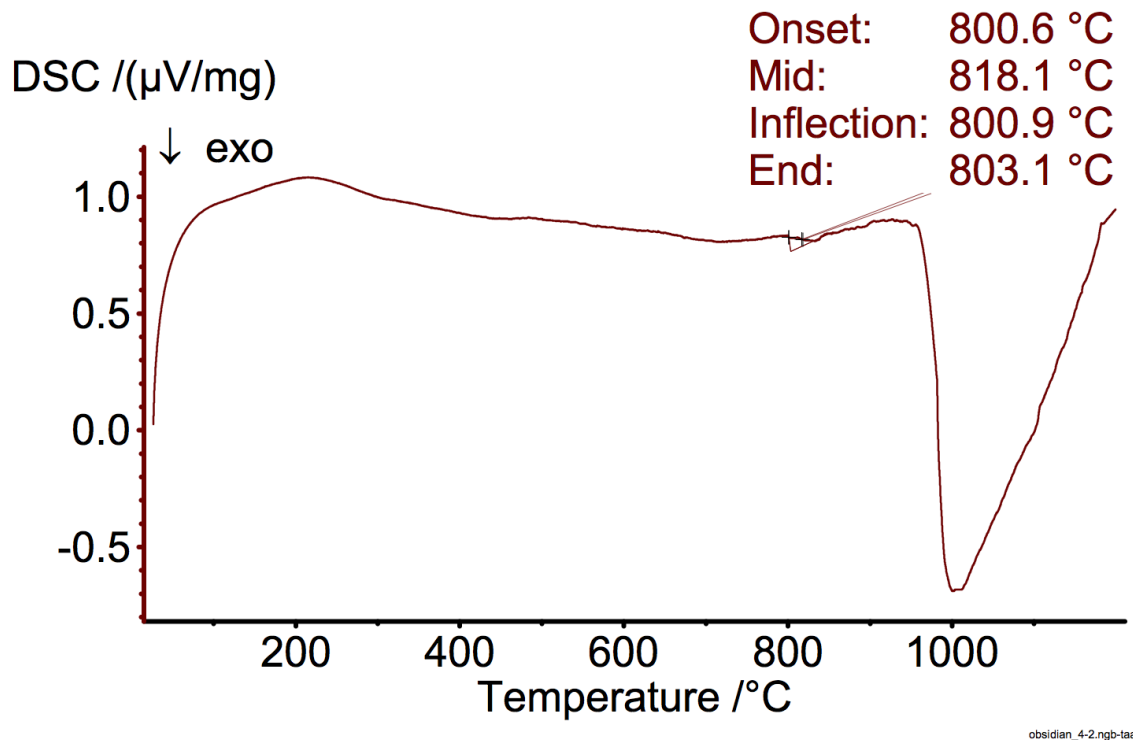


Figure III.16: DSC analysis of obsidian

III.6 Effect of Residual Stresses

To quantify the role of residual stresses in obsidian, a Vickers indent was introduced as a defect in obsidian. Kese *et al.* observed the influence of stress on measured mechanical properties of soda-lime glass with the help of vickers defect [?]. The Vickers indented samples were thermally annealed to two different temperatures with the aim of relieving stresses. The samples were brought back to room temperature and nanoindentation was performed around the Vickers indent at an angle of 45 degrees.

Figure ?? shows a SEM image of the obsidian surface after nanoindentation. Two temperatures were chosen in such a way that, one temperature was below T_g (500°C)

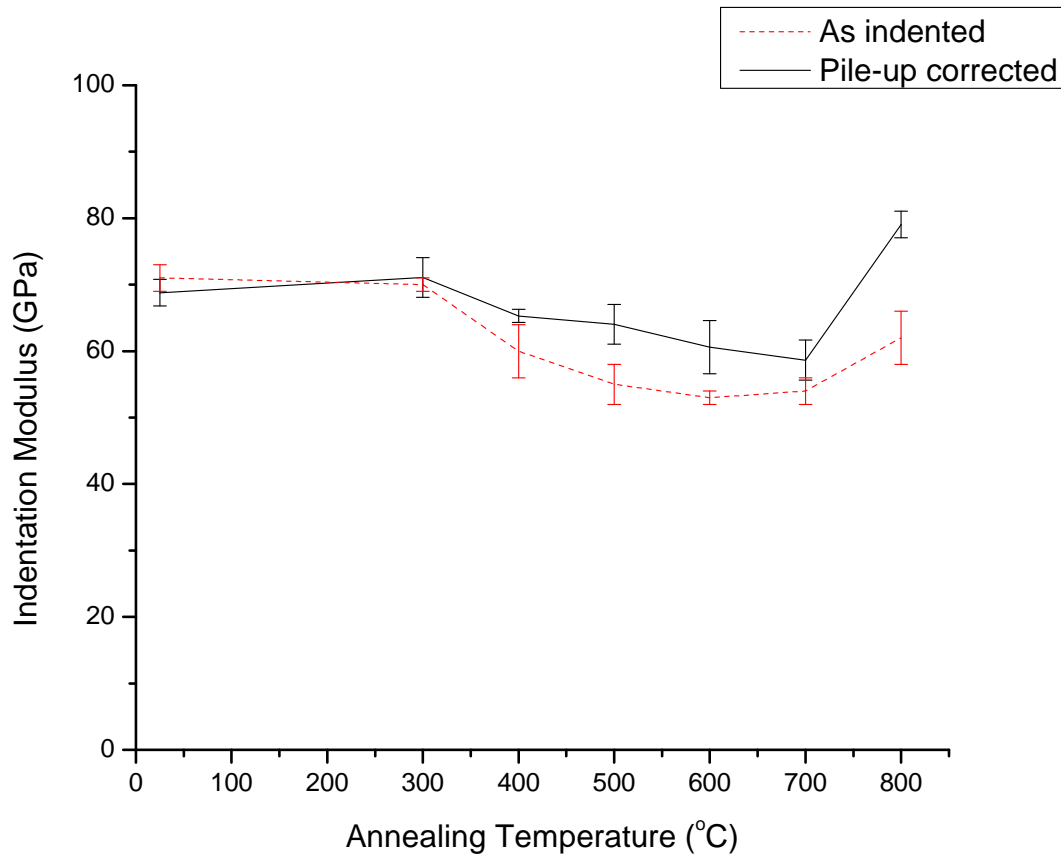


Figure III.17: Apparent Indentation modulus after area correction

and another was above T_g (800°C). Figure ?? shows the variation of apparent elastic modulus with distance from the vickers indentation for 500°C whereas figure ?? shows the same for 800°C . It can be observed that the apparent elastic modulus increases as the distance from the indenter and it can be seen that the apparent elastic modulus has also changed with soaking conditions. The elastic modulus of obsidian being higher around 800°C , to understand this behavior better, the residual stresses in obsidian have been calculated. Using the relation ?? between elastic modulus and residual stresses developed

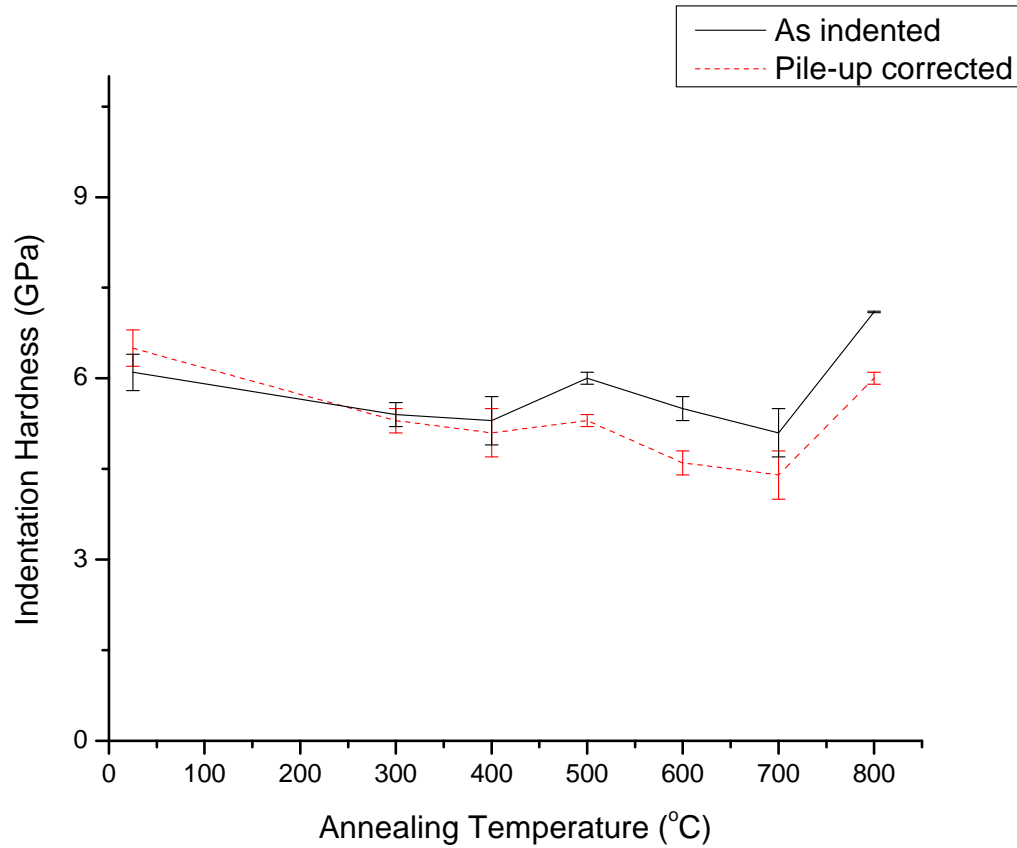


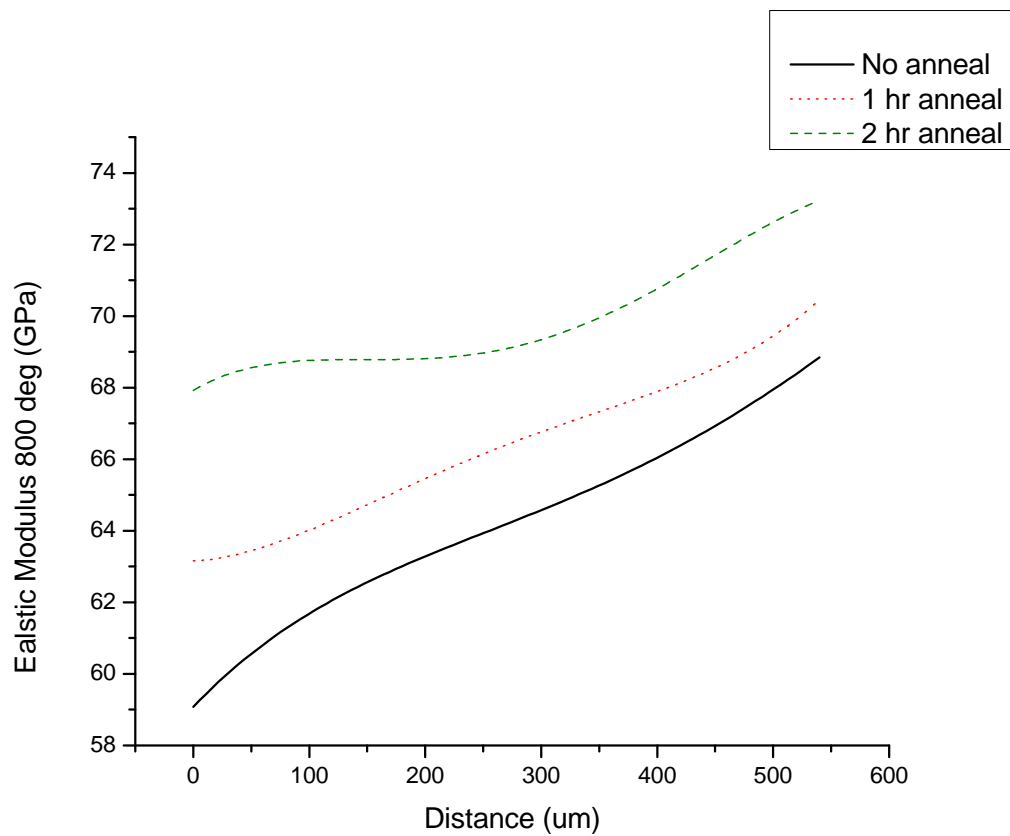
Figure III.18: Apparent Indentation hardness after area correction

by Mallinder and Proctor a fourth power polynomial fit was applied to the obtained data [?]. Figures ?? and ?? show the variation of residual stresses for different hold times across the stress field. The distance x , from the edge of the indent is normalized with respect to size, d , of the indent.

beginfigure[htb]



Figure III.19: SEM: Nanoindentations around vickers Indent



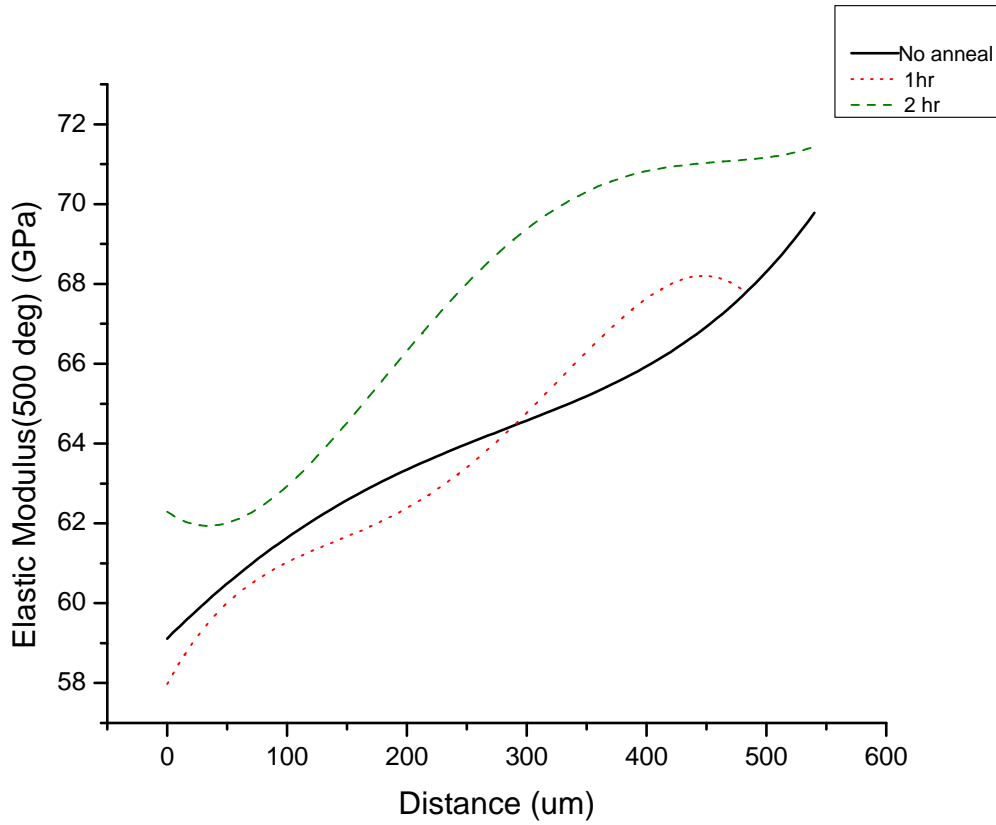


Figure III.20: Variation of apparent elastic modulus with distance from the indenter

Variation of apparent elastic modulus with distance from the indenter

$$\sigma \approx \frac{1}{10.22E_o}(E_o^2 - E^2) \quad \text{(III.2)}$$

The above graphs shows that residual stress reduction is higher at a temperature near T_g for a shorter soaking time. It can also be inferred that stresses are higher at the edge of the indent and decrease away from it. Such a behavior was also observed in aluminum alloys and different type of glasses. The only difference between obsidian and soda-lime glass is

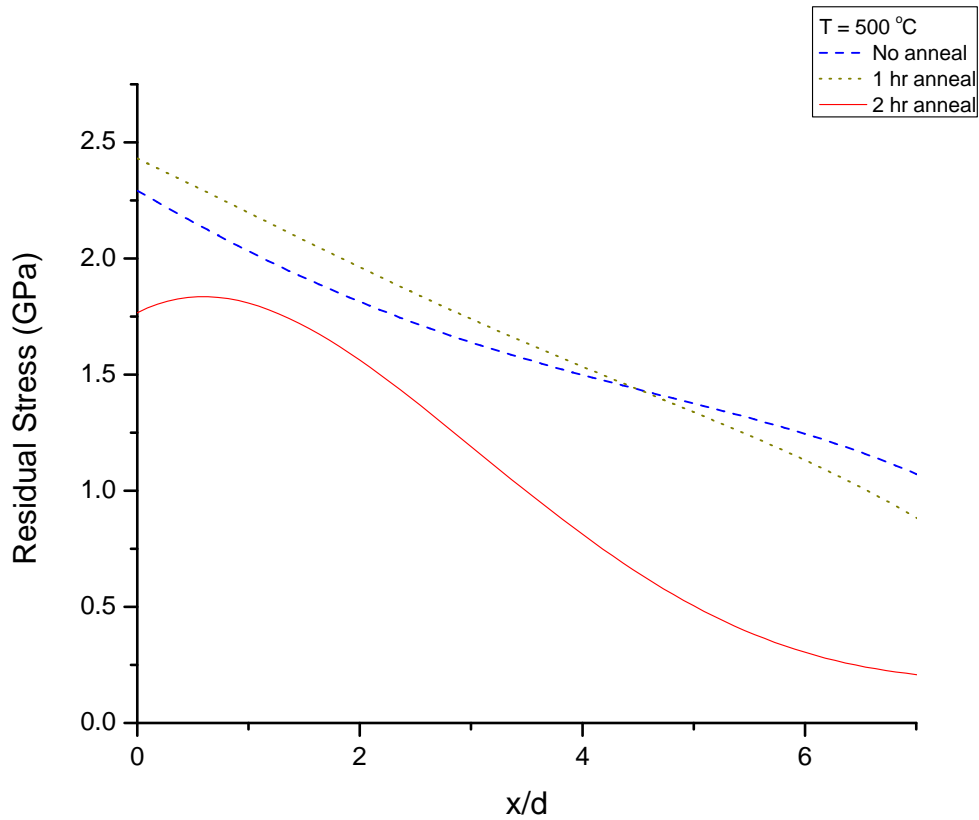


Figure III.21: Residual stresses variation in obsidian annealed at 500°C

that obsidian can withstand very high temperatures whereas glass melts at around 730 °C. The assumed stress relief is due to the decrease of plasticity in obsidian. The temperature above and near T_g has higher activation energies and are generally responsible for greater structural equilibrium. Complete stress relaxation may be achieved at a temperature below T_g for soda-lime glass if it is thermally annealed for more than 24 hours [?]. The same may be the case for obsidian too. This study infers that the mechanical properties are affected both by T_g and soaking time during thermal annealing, which changes the amount

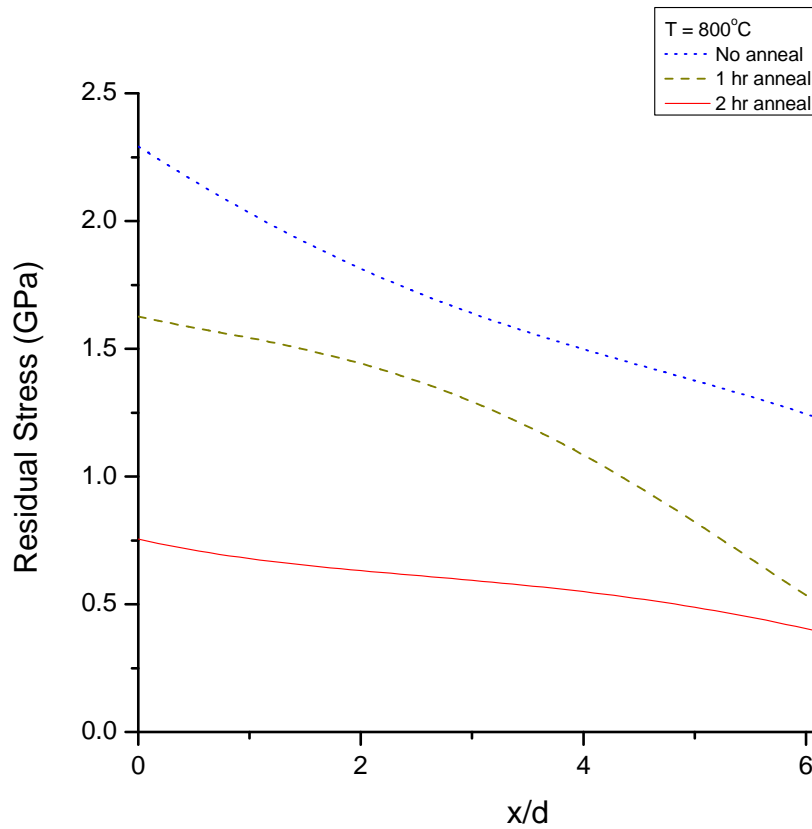


Figure III.22: Residual stresses variation in obsidian annealed at 800°C

of residual stress in the material. Although this method cannot resolve the residual stress field into its components and it is not yet clear how the tensile and compressive stresses combine to produce the desired results. These experiment shows that at these temperatures the residual stresses in obsidian relax.

CHAPTER IV

CONCLUSION AND FUTURE WORK

IV.1 Conclusion

Comparative examination of obsidian with soda-lime glass shows distinctive mechanical behavior. Nanoindentation results show that hardness of obsidian is higher than that of soda-lime glass. The mechanical properties were corrected for pile-up and a decrease in apparent modulus and apparent hardness was observed. Spectral analysis concludes the presence of alumina in obsidian, this allows obsidian to be an alumino-silicate glass. Presence of Fe in obsidian's composition can be interpreted for its black color. Thermal annealing of obsidian at different temperatures shows an apparent decrease in elastic modulus which might be due to the presence of residual stresses. The apparent indentation modulus and hardness after annealing were corrected for pile-up and sink-in behavior. The decrease in elastic modulus below T_g can be due to the fact that there might not be complete release of residual stresses or there might be dominance of tensile stresses in obsidian. It is speculated that residual stresses depend both on the annealing temperature and soaking time.

There cannot be a single reason for obsidian's superior mechanical properties. Through this study it is speculated that residual stress play a vital role in deciding obsidian's mechanical properties. It is not yet clear if the pre-induced stresses in obsidian upon rapid

cooling are either tensile or compressive. More understanding of the thermal history of obsidian gives us insight into the mechanical properties.

IV.2 Future Work

There are a few things which can be addressed to further understand the role of residual stresses of obsidian more clearly; they are:

- Understanding the yield strength of obsidian at different annealing temperatures, will help in comprehending the behavior of obsidian without the effect of contact area. This can be done from spherical indentation test.
- Quantifying the residual stresses in glass by the means of a polarimeter based on the principles developed by Jessop *et al.* [1]. The equation (1) used for finding out stresses is only an approximate one as it considers only uniaxial stresses.
- A clearer picture would be obtained if a series of finite element simulations are performed to carefully examine how stress influences the indentation process in obsidian and compare them to the experimental methods.

BIBLIOGRAPHY

- [1] A. Srivastava and R. Mirshams, “Microstructure and pile-up effect on nanoindentation measurements of FCC and BCC metals,” *NSTI - Nanotech*, vol. 4, 2007.
- [2] P. Moorey, *Ancient mesopotamian materials and industries*. Eisenbrauns, 1999.
- [3] E. A. Carter, M. D. Hargreaves, N. Kononenko, I. Graham, H. G. Edwards, B. Swarbrick, and R. Torrence, “Raman spectroscopy applied to understanding prehistoric obsidian trade in the pacific region,” *Vibrational Spectroscopy*, vol. 50, no. 1, pp. 116 – 124, 2009. {PROMINENT} {YOUNG} {VIBRATIONAL} {SPECTROSCOPISTS} 2009.
- [4] L. E. Morgan, P. R. Renne, R. E. Taylor, and G. WoldeGabriel, “Archaeological age constraints from extrusion ages of obsidian: Examples from the Middle Awash, Ethiopia,” *Quaternary geochronology*, vol. 4, pp. 193–203, June 2009.
- [5] A. J. Nazaroff, K. M. Prufer, and B. L. Drake, “Assessing the applicability of portable X-ray fluorescence spectrometry for obsidian provenance research in the maya lowlands,” *Journal of Archaeological Science*, vol. 37, no. 4, pp. 885 – 895, 2010.
- [6] J. A. O’Keefe, “Natural glass,” *Journal of Non-Crystalline Solids*, vol. 67, pp. 1–17, Dec. 1984.

- [7] W. Haviland, H. Prins, D. Walrath, and B. McBride, *Anthropology: The Human Challenge*. Cengage Learning, 13 ed., 2010.
- [8] B. A. Buck, “Ancient technology in contemporary surgery,” *West journal of medicine*, pp. 265–269, March 1982.
- [9] P. D. Sheets, “Dawn of a new stone age in eye surgery.,” *In Applying Anthropology: An Introductory Reader*, pp. 111–113, 1989.
- [10] J. Disa, “A comparison of obsidian and surgical steel scalpel wound healing in rats,” *Plastic and reconstructive surgery*, vol. 92, pp. 884–887, 10 1993.
- [11] A. Dalakishvili, “Glass formation in perlite- and obsidian-containing batches,” *Glass physics and chemistry*, vol. 31, pp. 820–822, Nov-Dec 2005.
- [12] A. Negash, M. Alene, F. H. Brown, B. P. Nash, and M. S. Shackley, “Geochemical sources for the terminal Pleistocene/early Holocene obsidian artifacts of the site of Beseka, central Ethiopia,” *Journal of archaeological science*, vol. 34, pp. 1205–1210, Aug 2007.
- [13] W. George, “Obsidian,” *Journal of Geology*, 1924.
- [14] J. Ericson, A. Makishima, J. Mackenzie, and R. Berger, “Chemical and physical properties of obsidian: a naturally occurring glass,” *Journal of Non-Crystalline Solids*, vol. 17, no. 1, pp. 129 – 142, 1975.
- [15] U. Gerth and J. Schnapp, “Investigation of mechanical properties of natural glasses

- using indentation methods,” *Chemie der erde-Geochemistry*, vol. 56, pp. 398–403, DEC 1996. 3rd Conference on Natural Glasses, Jena, Germany, March, 1996.
- [16] B. Dorfman, Skinner, S. C.E.; Zunjarrao, and R. Singh, “Obsidian - Natural Nanostructured Glass: Preliminary Research Results ,” in *Proceedings of the XIth international congress and exposition*, 2008.
- [17] Husien, “Fracture behavior and mechanical characterization of obsidian: Naturally occurring glass,” Master’s thesis, Oklahoma State University, 2010.
- [18] Matsushima.S.; “Elastic modulus of volcanic glass, glassy rocks and crystalline rocks to 1000 degrees and 20 Kbar,” in *International Geodynamics Conference*, 1978.
- [19] T. Murase, “A note on visco-elastic behavior of obsidian,” *Journal of the faculty of science*, vol. I, no. 2, pp. 103–113, 1958.
- [20] S. Kaichi, M. Makoto, S. Tetsuya, and F. Hideyuki, “Elastic properties of obsidian, vitreous SiO₂, and vitreous GeO₂ under high pressure up to 6 GPa,” *Geophysical monograph series*, vol. 67, pp. 219–225, 1992.
- [21] H. Ben Abdelounis, K. Elleuch, R. Vargiolu, H. Zahouani, and A. Le Bot, “On the behavior of obsidian under scratch test,” *Wear*, vol. 266, pp. 621–626, Mar 25 2009.
- [22] C. Ma, G. R. Rossman, and J. A. Miller, “The origin of color in “fire” obsidian,” *Canadian Mineralogist*, vol. 45, pp. 551–557, Jun 2007.
- [23] M. L. Janine, M. O. Thomas, and F. David A, “The effects of fire and heat on obsidian,” in *Annual meeting of society for california archaeology*, 1999.

- [24] S. Kolzenburg, J. K. Russell, and L. A. Kennedy, “Energetics of glass fragmentation: Experiments on synthetic and natural glasses,” *Geochemistry, Geophysics, Geosystems*, vol. 14, no. 11, pp. 4936–4951, 2013.
- [25] M. S. Shackley and C. Dillian, “Thermal and environmental effects on obsidian geochemistry: experimental and archaeological evidence,” *The effects of fire and heat on obsidian*, pp. 117–134, 2002.
- [26] R. A. Wilson and H. A. Bullen, “Introduction to Scanning Probe Microscopy (SPM) basic theory Atomic Force Microscopy (AFM),” tech. rep., Department of Chemistry, Northern Kentucky University, Highland Heights, KY 41099, 2007.
- [27] X. Li and B. Bhushan, “A review of nanoindentation continuous stiffness measurement technique and its applications,” *Materials Characterization*, vol. 48, no. 1, pp. 11 – 36, 2002.
- [28] K. Kwadwo, T. Matilda, and B. Bergman, “Contact residual stress relaxation in soda-lime glass: Part i. measurement using nanoindentation,” *Journal of the European Ceramic Society*, vol. 26, no. 6, pp. 1003 – 1011, 2006.
- [29] J. Hay and W. Oliver, “Using the ratio of loading slope and elastic modulus to predict pile-up and constraint factor during indentation,” *material research society*, vol. 522, 1988.
- [30] J. Tuck, A. Korsunsky, S. Bull, and R. Davidson, “On the application of the work-of-indentation approach to depth-sensing indentation experiments in coated systems,” *Surface & Coatings technology*, vol. 137, pp. 217–224, MAR 15 2001.

- [31] J.E.Shelby, *Introduction to glass science and technology*. Royal society of chemistry, 2005.
- [32] M. S. Gaafar and S. Y. Marzouk, “Mechanical and structural studies on sodium borosilicate glasses doped with Er_2O_3 using ultrasonic velocity and FTIR spectroscopy,” *Physica B-condensed matter*, vol. 388, pp. 294–302, JAN 15 2007.
- [33] D. L. Pavia, *Introduction to spectroscopy*. Belmont, CA: Brooks/Cole, Cengage Learning, 2009.
- [34] A. Bolshakov and G. Pharr, “Influences of pile-up on the measurement of mechanical properties by load and depth sensing indentation techniques,” *Journal of material research*, vol. 13, pp. 1049–1058, APR 1998.
- [35] K. Kese, Z. Li, and B. Bergman, “Influence of residual stress on elastic modulus and hardness of soda-lime glass measured by nanoindentation,” *Journal of materials research*, vol. 19, pp. 3109–3119, OCT 2004.
- [36] J. Shen, D. J. Green, R. E. Tressler, and D. L. Shelleman, “Stress relaxation of a soda lime silicate glass below the glass transition temperature,” *Journal of Non-Crystalline Solids*, vol. 324, no. 3, pp. 277 – 288, 2003.
- [37] G. Pharr, T. Tsui, A. Bolshakov, and W. Oliver, “Effects of residual stress on the measurement of hardness and elastic modulus using nanoindentation,” in *Symposium – Materials Reliability in Microelectronics IV*, vol. 338 of *MRS Online Proceedings Library*, 1 1994.

- [38] T. Y. Tsui, W. C. Oliver, and G. M. Pharr, "Influences of stress on the measurement of mechanical properties using nanoindentation: Part i. experimental studies in an aluminum alloy," *Journal of Materials Research*, vol. 11, pp. 752–759, 3 1996.
- [39] A. Bolshakov, W. C. Oliver, and G. M. Pharr, "Influences of stress on the measurement of mechanical properties using nanoindentation: Part II. finite element simulations," *Journal of Materials Research*, vol. 11, pp. 760–768, 3 1996.
- [40] J. C. Hay, A. Bolshakov, and G. M. Pharr, "A critical examination of the fundamental relations used in the analysis of nanoindentation data," *Journal of Materials Research*, vol. 14, pp. 2296–2305, 6 1999.
- [41] J. Frankel, A. Abbate, and W. Scholz, "The effect of residual stresses on hardness measurements," *Experimental Mechanics*, vol. 33, no. 2, pp. 164–168, 1993.
- [42] K. McElhaney, J. Vlassak, and W. Nix, "Determination of indenter tip geometry and indentation contact area for depth-sensing indentation experiments," *Journal of materials research*, vol. 13, pp. 1300–1306, May 1998.
- [43] F. Mallinder and B. Proctor, "Elastic constants of fused silica as a function of large tensile strain," *Phys. Chem. Glasses*, vol. 5, pp. 91–103, 1964.
- [44] H. Jessop, "On the tardy and senarmont methods of measuring fractional relative retardations," *British journal of applied physics*, vol. 4, no. May, pp. 138–141, 1953.

VITA

RAGHU V MEESALA

Candidate for the Degree of

Master of Science

Thesis: ROLE OF RESIDUAL STRESSES ON MECHANICAL PROPERTIES OF OB-
SIDIAN: NATURALLY OCCURRING GLASS

Major Field: Mechanical and Aerospace Engineering

Biographical:

Personal Data: Born in Hyderabad, India on September 9 , 1988.

Education:

Received the B.E. degree from Osmania University, Hyderabad, India, 2010,
in Mechanical Engineering

Completed the requirements for the degree of Master of Science with a major in
Mechanical and Aerospace Engineering at Oklahoma State University in July,
2014.

Experience:

Graduate Research Assistant in Mechanics of Advanced Materials Laboratory,
Oklahoma State University

Graduate Teaching Assistant, Oklahoma State University